



# OsmiR528 regulates rice-pollen intine formation by targeting an uclacyanin to influence flavonoid metabolism

Yu-Chan Zhang<sup>a</sup>, Rui-Rui He<sup>a</sup>, Jian-Ping Lian<sup>a</sup>, Yan-Fei Zhou<sup>a</sup>, Fan Zhang<sup>a</sup>, Quan-Feng Li<sup>a</sup>, Yang Yu<sup>a</sup> , Yan-Zhao Feng<sup>a</sup> , Yu-Wei Yang<sup>a</sup>, Meng-Qi Lei<sup>a</sup>, Huang He<sup>a</sup>, Zhi Zhang<sup>a</sup>, and Yue-Qin Chen<sup>a,1</sup>

<sup>a</sup>Guangdong Provincial Key Laboratory of Plant Resources, State Key Laboratory for Biocontrol, Sun Yat-Sen University, 510275 Guangzhou, People's Republic of China

Edited by David C. Baulcombe, University of Cambridge, Cambridge, United Kingdom, and approved November 27, 2019 (received for review June 27, 2018)

The intine, the inner layer of the pollen wall, is essential for the normal development and germination of pollen. However, the composition and developmental regulation of the intine in rice (*Oryza sativa*) remain largely unknown. Here, we identify a microRNA, OsmiR528, which regulates the formation of the pollen intine and thus male fertility in rice. The *mir528* knockout mutant aborted pollen development at the late binucleate pollen stage, significantly decreasing the seed-setting rate. We further demonstrated that OsmiR528 affects pollen development by directly targeting the uclacyanin gene *OsUCL23* (encoding a member of the plant-specific blue copper protein family of phytocyanins) and regulating intine deposition. *OsUCL23* overexpression phenocopied the *mir528* mutant. The OsUCL23 protein localized in the prevacuolar compartments (PVCs) and multivesicular bodies (MVBs). We further revealed that OsUCL23 interacts with a member of the proton-dependent oligopeptide transport (POT) family of transporters to regulate various metabolic components, especially flavonoids. We propose a model in which OsmiR528 regulates pollen intine formation by directly targeting *OsUCL23* and in which OsUCL23 interacts with the POT protein on the PVCs and MVBs to regulate the production of metabolites during pollen development. The study thus reveals the functions of OsmiR528 and an uclacyanin during pollen development.

pollen | intine | miRNA | uclacyanin | rice

The pollen wall is a complex multilayered structure on the outer surface of pollen grains that consists of an outer exine layer and an internal intine layer in most species (1). The intine layer, which is located between the exine of the pollen wall and the cell membrane, is essential for the maturation of the pollen grain and pollen tube germination. The intine usually starts to develop under the control of many factors such as flavonols (2) at the vacuolated stage and is believed to have a composition similar to the plant primary cell walls, which contain cellulose, hemicellulose, pectic substances, and hydrophobic proteins (1). Most of the progress in understanding the composition of the intine and the molecular mechanisms behind its development has been made in the study of model plant *Arabidopsis thaliana* (1, 3, 4). In the major crop species rice (*Oryza sativa*), however, our knowledge of the intine is very limited (5, 6). Given the importance of the intine for pollen grain maturation and pollen tube germination, as well as for the pollination of crops, the identification of the regulators of intine formation is vital for enhancing our understanding of these processes, especially for crop breeding.

Phytocyanins are part of the blue copper protein family and include stellacyanins, plantacyanins, uclacyanins, and early nodulin group subfamilies (7). So far, most of the research on phytocyanins has focused on their biochemical, spectroscopic, and redox properties, although some studies have demonstrated that plantacyanins are closely involved in the reproductive development of plants (8, 9). The messenger RNAs (mRNAs) encoding several uclacyanins have been shown to be targeted by

2 regulatory microRNAs (miRNAs) in rice, OsmiR408 and OsmiR528 (10, 11). OsmiR528 is a conserved monocot-specific miRNA, which has been reported to play multifaceted roles in various developmental processes such as regulating plant responses to biotic and abiotic stress (12–15) and regulating flowering time (16). Importantly, OsmiR528 was found to be differentially expressed in fertile and sterile rice lines (17), suggesting that it might be involved in the regulation of fertility; however, the role of OsmiR528 and uclacyanins in rice fertility is totally unknown.

In this study, we report the role of OsmiR528 and its target, *OsUCL23* (encoding a member of the uclacyanin family), in regulating pollen intine development and thus the seed-setting rate in rice. We further demonstrate that OsmiR528 affects pollen development by directly targeting *OsUCL23* at the binucleate pollen stage. *OsUCL23* regulates the deposition of the pollen intine by interacting with a proton-dependent oligopeptide transport (POT) transporter in prevacuolar compartment (PVC)/multivesicular bodies (MVBs). We have therefore revealed OsmiR528 functioning in pollen grain development.

## Results

### Loss-of-Function in OsmiR528 Causes Aberrant Male Gametogenesis.

To determine if OsmiR528 is involved in plant reproductive growth, we obtained a rice T-DNA insertion mutant (Fig. 1A), *mir528* (PFG\_1B-10308.L), from the Korean Postech database (18). *pri-miR528*, *pre-miR528*, and OsmiR528 were undetectable in this mutant (Fig. 1B). We also generated OsmiR528 overexpression

## Significance

The intine layer of pollen is essential for pollen grain maturation and pollen tube germination. Abnormal intine development causes pollen sterility and affects seed-setting; therefore, the identification of regulators of intine formation is important for elucidating the mechanisms of pollen formation and function, especially for crop breeding. Here, we report a microRNA, OsmiR528, which regulates pollen intine formation and male fertility in rice (*Oryza sativa*). OsmiR528 directly targets the uclacyanin family member *OsUCL23* to regulate flavonoid metabolism and pollen intine development. This study revealed the function of OsmiR528 and an uclacyanin in pollen development.

Author contributions: Y.-C.Z. and Y.-Q.C. designed research; Y.-C.Z., R.-R.H., J.-P.L., Y.-F.Z., F.Z., Q.-F.L., Y.-Z.F., Y.-W.Y., and M.-Q.L. performed research; Y.-C.Z., R.-R.H., J.-P.L., Y.-F.Z., F.Z., Q.-F.L., Y.Y., Y.-Z.F., H.H., Z.Z., and Y.-Q.C. analyzed data; and Y.-C.Z., Y.Y., and Y.-Q.C. wrote the paper.

The authors declare no competing interest.

This article is a PNAS Direct Submission.

This open access article is distributed under Creative Commons Attribution-NonCommercial-NoDerivatives License 4.0 (CC BY-NC-ND).

<sup>1</sup>To whom correspondence may be addressed. Email: lsscyq@mail.sysu.edu.cn.

This article contains supporting information online at <https://www.pnas.org/lookup/suppl/doi:10.1073/pnas.1810968117/-DCSupplemental>.

First published December 23, 2019.

lines (OXmiR528, expression levels shown in Fig. 1C). The phenotypes of *mir528* and OXmiR528 plants were then analyzed from the vegetative stage to the reproductive stage. The *mir528* mutants were slightly shorter than the wild-type (WT) plants (SI Appendix, Fig. S1A and B), and their panicles were semisterile (Fig. 1D and E). Conversely, the OXmiR528 plants had a higher seed-setting rate (Fig. 1D and E), suggesting that OsmiR528 might be involved in the regulation of fertility.

We next analyzed floral development in the mutant plants to identify how OsmiR528 affects fertility. The phenotypic analysis showed that both the *mir528* and OXmiR528 plants developed normal pistils and anthers (SI Appendix, Fig. S1C), but iodine-potassium iodide staining revealed that *mir528* plants have significantly more aborted pollen grains whereas OXmiR528 plants have fewer aborted pollen grains than WT plants (Figs. 1F and 2A). To identify the exact stage at which the mutant pollen grains began to show phenotypic defects, we compared WT, OXmiR528, and *mir528* pollen in paraffin (SI Appendix, Fig. S1D) and semithin sections (SI Appendix, Fig. S2A). At the pollen mother-cell stage, meiosis stage, and the young microspore stage, the pollen grains of OXmiR528 plants and the *mir528* mutant were similar to that of the WT plants; however, at the late binucleate pollen stage and mature stage, half of the *mir528* pollen grains had shrunk and had no cytosolic content (SI Appendix, Fig. S2A). These results showed that OsmiR528 is essential for pollen grain maturation.

**OsmiR528 Regulates Pollen Intine Formation.** Next, we investigated which process was regulated by OsmiR528 during pollen development by examining the mature pollen grains of WT, OXmiR528, and *mir528* plants. Three staining methods (Alexander's staining, auramine O staining, and calcofluor white staining) were applied to detect pollen viability, the pollen exine, and the pollen intine, respectively. As shown in Fig. 2A, the defective pollen grains in the *mir528* mutant were not viable. The pollen grains of the

mutant, including aborted pollen grains, had an intact exine; however, the defective pollen from the *mir528* mutants exhibited very weak calcofluor white staining relative to that in the WT pollen grains (Fig. 2A), indicating that the intine might be defective in the mutant pollen. Statistical analysis showed that *mir528* plants presented more nonviable, intine-defective pollen grains, whereas OXmiR528 plants presented fewer nonviable, intine-defective pollen grains than WT plants (Fig. 2B), and the heterozygous *mir528* plants showed intermediate phenotypes (SI Appendix, Fig. S2B and C). The intine was previously reported to be essential for pollen germination and pollen tube elongation on the stigma (19); therefore, we next monitored pollen tube germination in the mutant, the overexpressor line, and WT plants (SI Appendix, Fig. S2D). The pollen grains germinated on the stigma 2 h after anthesis in the WT plants and OXmiR528, whereas very few *mir528* pollen grains germinated. We also performed an in vitro pollen germination experiment to investigate the effects of OsmiR528 on the germination rates (SI Appendix, Fig. S2E). As shown in Fig. 2C, *mir528* plants showed a significantly lower rate than that in WT plants, whereas OXmiR528 plants had a higher rate than that in WT plants. These results show that OsmiR528 is involved in pollen intine formation, which in turn affects pollen germination.

To understand how intine development was affected in the mutants, we used transmission electron microscopy to examine the pollen at the early microspore stage (EMS), vacuolated pollen stage (VPS), early binucleate pollen stage (EBPS), late binucleate pollen stage (LBPS), and MPS (Fig. 3A and SI Appendix, Fig. S3). At EMS and VPS, both the WT and mutant plants developed an exine layer, while the intine was unobservable (SI Appendix, Fig. S3). At EBPS, the intine started to accumulate, and at LBPS, OXmiR528 exhibited a higher accumulation rate than WT and *mir528* plants, but approximately half of the microspores in *mir528* plants could not initiate intine formation, and the phenotypes became more apparent at MPS; thus, half of the pollen grains were totally defective in intine accumulation (Fig. 3A). We further analyzed the intine thickness of the normally developed pollen grains in the mutants and WT plants; the aborted pollen grains, which accounted for over half of the pollen grains in *mir528* plants, which presented no intine, were not included in the statistical analysis to avoid biased results. Significant differences in intine thickness between the mutants and WT plants were observed from LBPS to MPS (Fig. 3B). OXmiR528 plants exhibited significantly thicker intines than WT pollen, whereas the normally developed *mir528* pollen exhibited thinner intines than WT pollen, and the aborted pollen grains contained no starch and exhibited a severe defect in their intine layer (Fig. 3B). Previous research suggested that intine development precedes the accumulation of pollen grain inclusions such as starch (20); we therefore speculate that OsmiR528 positively regulates pollen intine formation during late gametogenesis, which affects fertility.

**OsmiR528 Targets an mRNA Encoding a Uclacyanin Protein to Regulate Pollen Grain Development.** To investigate how OsmiR528 regulates pollen grain maturation, we analyzed the potential targets of this microRNA. The mRNAs of several genes are potential targets of OsmiR528 in rice, including genes encoding an ascorbic acid oxidase (LOC\_Os06g37150), a laccase (LOC\_Os01g62600), a D3 protein (LOC\_Os06g06050), and a member of the uclacyanin family (*OsUCL23*, LOC\_Os08g04310) (10). The gene encoding the ascorbic acid oxidase was previously reported to be involved in the biotic- and abiotic-stress responses, but was not found to affect reproductive growth (12–14). The laccase gene (LOC\_Os01g62600) was expressed at an extremely low level (SI Appendix, Fig. S4A). We excluded these 2 genes from the analysis and focused on the D3 gene and *OsUCL23*. The function of *OsUCL23* has not yet been elucidated. D3 was known to control tillering by suppressing axillary bud activity (21). The mRNA abundances of both *OsUCL23* and D3 were down-regulated in the OXmiR528 plants and up-regulated in the *mir528* mutants (SI Appendix, Fig. S4A and B), indicating that their expression levels are negatively correlated with that of OsmiR528. We then constructed overexpression lines of *OsUCL23*

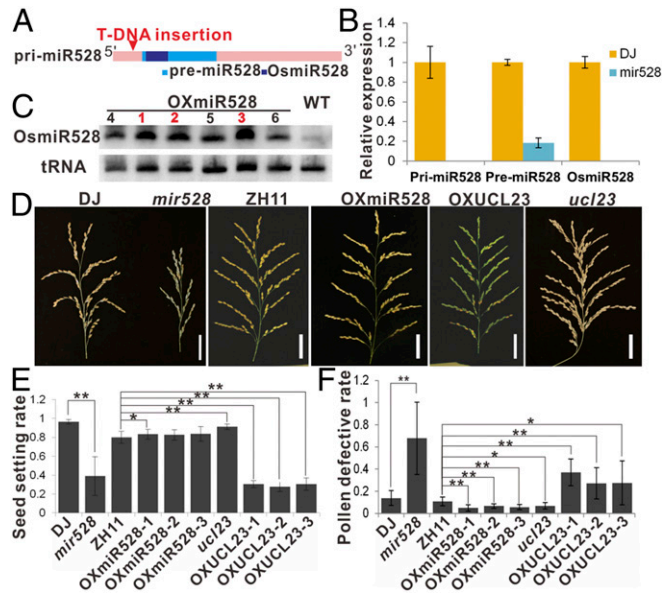


**Fig. 1.** OsmiR528 and *OsUCL23* are involved in pollen grain maturation. (A) Schematic representation of the OsmiR528 gene structure and the T-DNA insertion site in the *mir528* mutant. (B) Relative expression levels of Pri-, Pre-, and mature OsmiR528 in *mir528* mutants and DJ WT panicles. (C) Abundance of OsmiR528 in the panicles of multiple independent OXmiR528 lines, and lines 1, 2, and 3, which are indicated in red, were used in the following study. (D) Panicles of WT and mutant plants at the mature stage. (Scale bars, 4 cm.) (E) Seed-setting rates of different transgenic plants. Values shown are the means  $\pm$  SD ( $n > 20$  plants). Significant differences were identified using Student's *t* test. (F) Ratio of defective pollen grains in different transgenic plants. Values shown are the means  $\pm$  SD ( $n > 10$  plants, 200 pollen grains). Significant differences were identified using Student's *t* test. \**P* < 0.05, \*\**P* < 0.01.

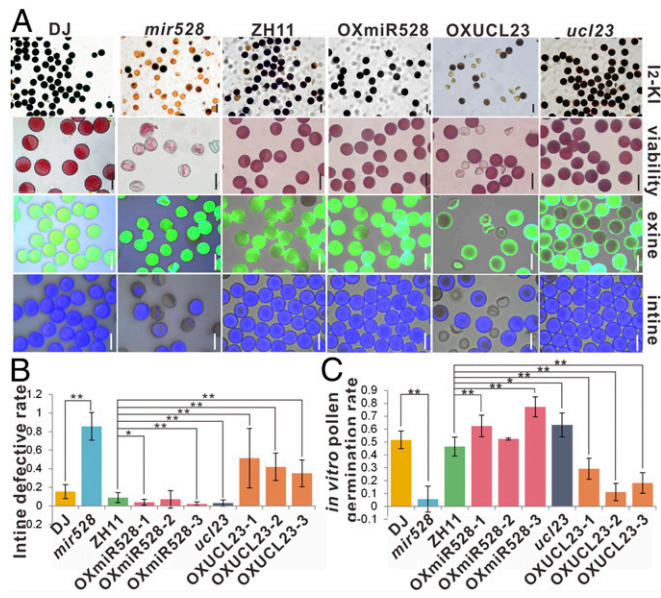


**Fig. 2.** OsmiR528 is required for pollen grain maturation and pollen tube germination. (A) Histochemical staining of WT and mutant pollen grains showed a defect in pollen grain maturation and intines of the *mir528* and OXUCL23 plants. (Scale bars, 50  $\mu\text{m}$ .) (B) Ratio of pollen grains with defective intines in different transgenic plants. Values shown are the means  $\pm$  SD ( $n > 10$  plants, 200 pollen grains). Significant differences were identified using Student's *t* test. (C) In vitro pollen germination rates of different transgenic plants. Values shown are the means  $\pm$  SD ( $n > 200$  pollen grains). Significant differences were identified using Student's *t* test. \* $P < 0.05$ , \*\* $P < 0.01$ .

(OXUCL23) and *D3* (OXD3) and analyzed their phenotypes (*SI Appendix, Fig. S4 B and C*). The OXUCL23 plants, but not the OXD3 plants, had a decreased seed-setting rate (Fig. 1 *D and E* and *SI Appendix, Fig. S4 D and E*), which phenocopied *mir528*, suggesting that OsmiR528 regulates seed-setting by downregulating *OsUCL23* but not *D3*. We further monitored the cleavage by OsmiR528 on *OsUCL23* mRNA using 5' rapid amplification of complementary DNA (cDNA) ends. The result showed that OsmiR528 cleaved *OsUCL23* mRNA between the 10th and 11th nucleotide, which is the traditional cleavage site of plant miRNAs (Fig. 4A).

We then constructed knockout mutant lines of *OsUCL23* (*ucl23*) using CRISPR-Cas9. The guide RNA was designed to target the first *OsUCL23* exon at the predicted signal peptide region adjacent to the OsmiR528 target site (Fig. 4A). A homozygous mutant with a 64-bp deletion at the signal peptide region, causing a frameshift and a loss of expression of WT *OsUCL23* transcript (Fig. 4A and *SI Appendix, Fig. S4B*), was developed for use in the following experiments.

We performed phenotypic analyses of the OXUCL23 plants and *ucl23* plants. The plant architecture and spikelets of both OXUCL23 and *ucl23* were similar to the WT plants (*SI Appendix, Fig. S1 A–C*); however, the panicles of the OXUCL23 plants were semisterile (Fig. 1 *D and E*). Iodine–potassium iodide staining revealed that half of the pollen grains of the OXUCL23 plants had no starch deposition (Figs. 1*F* and 2*A*). We then performed sectioning of the anthers of WT, OXmiR528, OXUCL23, and *ucl23* plants from the pollen mother-cell stage to the mature stage (*SI Appendix, Figs. S1D and S2A*), revealing no apparent differences between the anthers from the mutant or overexpressing plants and the WT anthers at the pollen mother-cell stage, meiosis stage, or early microspore stage (*SI Appendix, Figs. S1D and S2A*). At the mature stage however, only half of the OXUCL23 pollen grains were filled with starch, similar to the phenotype of the *mir528* pollen grains (*SI Appendix, Fig. S2A*), supporting the hypothesis that OsmiR528 regulates late microspore development by targeting *OsUCL23*.

We next applied Alexander's staining, auramine O staining, and calcofluor white staining to observe pollen grain viability and structure (Fig. 2*A*). While the WT and *ucl23* pollen grains emitted

bright blue fluorescence, the OXUCL23 pollen grains exhibited a very weak calcofluor white signal, similar to those of *mir528* plants, demonstrating that the intine was defective in OXUCL23 pollen (Fig. 2*A and B*). Transmission electron microscopy showed that the OXUCL23 pollen grains presented a similar exine to the WT and *ucl23* pollen grains, whereas the aborted pollen grains of OXUCL23 plants could not initiate intine formation at EBPS and exhibited no intine and starch accumulation at LBPS and MPS, while the other pollen grains presented a significantly thinner intine than the WT plants at MPS (Fig. 3*A and SI Appendix, Fig. S3*). The intine of the *ucl23* pollen grains was thicker than the WT intine, similar to that of the OXmiR528 plants (Fig. 3*A and B*). Consistent with these observations, in vivo and in vitro pollen grain germination was also repressed in OXUCL23 plants, whereas in vitro germination rates were higher in *ucl23* plants than in WT plants, indicating that their defective intine inhibits the germination of the OXUCL23 pollen tubes (Fig. 2*C and SI Appendix, Fig. S2 B–E*). We further analyzed the function of the female organs of OXUCL23 and *mir528* plants by crossing OXUCL23 plants with OXmiR528 plants and crossing *mir528* plants with DongJing (DJ) WT plants (OXUCL23 or *mir528* plants served as the male parent or female parent) (*SI Appendix, Fig. S5A*). As expected, we obtained more hybrids when using OXUCL23 or *mir528* as the female parent, while fewer hybrids were obtained when using OXUCL23 as the male parent, and no hybrids were obtained when using *mir528* as the male parent (*SI Appendix, Fig. S5 B and C*). The hybrids obtained using OXUCL23 or *mir528* as the male parent developed normal embryos (*SI Appendix, Fig. S5B*), which indicated that the pistils of the OXUCL23 and *mir528* plants were normally developed and that the decreased seed-setting rate in OXUCL23 and *mir528* plants was caused by aborted pollen grains and a decreased pollen grain germination rate. We concluded that OsmiR528 interacts with *OsUCL23* mRNA to promote its cleavage, which positively regulates pollen intine formation during late gametogenesis and consequently affects fertility.

**OsUCL23 Localizes to Prevacuolar Compartments and Multivesicular Bodies.** Above, we showed that OsUCL23 affects the formation of the pollen intine. Next, we investigated the mechanism that causes this effect. The OsUCL23 protein contains a 30-amino-acid (AA) signal peptide (the secretion signal) at its N terminus, a 33-AA glycosylphosphatidylinositol (GPI)-anchor signal at its C terminus, and a plastocyanin-like domain (Fig. 4A). To investigate the subcellular localization of the OsUCL23 protein, GFP was fused to the N-terminal, C-terminal, or central region of OsUCL23 as shown in the diagram (Fig. 4A). These fusion molecules were expressed under the control of the *Cauliflower mosaic virus* 35S promoter and were transformed into rice protoplasts. As the GPI anchor is often responsible for membrane localization (22), we coexpressed the endoplasmic reticulum (ER)-yellow fluorescent protein (YFP) marker CD3-958, the Golgi-YFP marker CD3-966, the nucleus-mCherry marker HY5, and the cytoplasm marker pUC-mCherry with the N-GFP-UCL23-C fusion protein in protoplasts to enable subcellular localization studies of the GFP-OsUCL23 constructs (*SI Appendix, Fig. S6*).

After incubating the transformed cells for 12 h, we monitored the localization of the fusion proteins using a confocal microscope. The fluorescent signals exhibited a spotty distribution, partially overlapping with the ER marker but not the Golgi marker (*SI Appendix, Fig. S6*). The distribution of OsUCL23 was similar to that of the organelles in the endomembrane system. We then determined whether OsUCL23 colocalized with the prevacuolar compartment and multivesicular body (PVC and MVB, respectively, which respond to brefeldin A) marker VSR2 or the trans-Golgi network (which responds to wortmannin) marker SYP61 (23–25). The fluorescence signals of GFP-OsUCL23 overlapped with the VSR2 marker but not with the SYP61 marker, indicating that OsUCL23 localizes to PVCs and MVBs (*SI Appendix, Fig. S6 and Fig. 4B*). We further analyzed the effect of different domains of OsUCL23 on its subcellular localization.

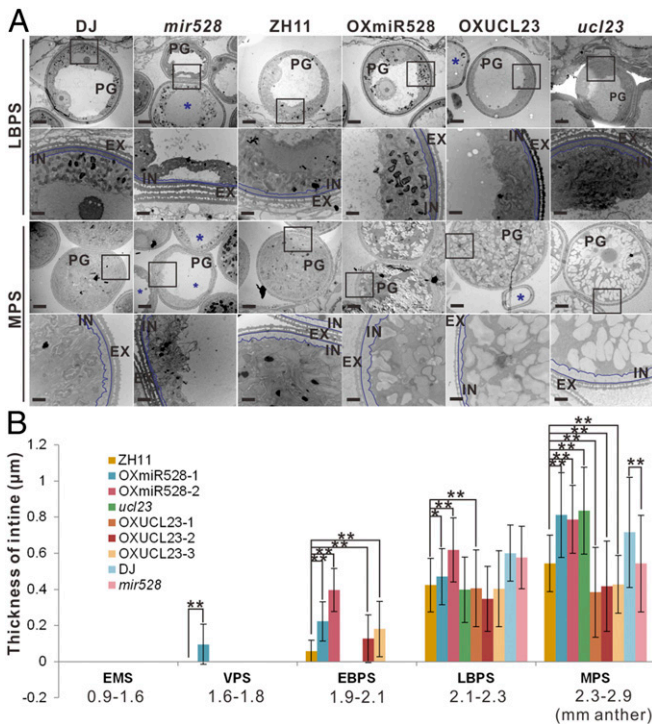


**Fig. 3.** OsmiR528 and OsUCL23 affect the intine thickness of mature pollen grains. (A) Transmission electron microscopy analysis of WT and mutant mature pollen grain intine layers at EBPS, LBPS, and MPS. (Lower) Magnifications of the outlined squares in the Upper panels. Aborted pollen grains are indicated by blue asterisks, and the intine is surrounded by blue lines. (Scale bars, 10  $\mu$ m for the Upper, 2  $\mu$ m for the magnified panels.) PG, pollen grains; EX, exine; IN, intine. (B) Thickness of the intines in WT and mutant pollen grains at the EMS, VPS, EBPS, LBPS, and MPS. Values shown are the means  $\pm$  SD ( $n > 3$  plants, 25 pollen). Significant differences were identified using Student's *t* test. \* $P < 0.05$ , \*\* $P < 0.01$ .

When the GFP protein was fused to different parts of OsUCL23, we found that both parts of the OsUCL23 protein give the fusion protein the ability to localize to PVC/MVBs (Fig. 4 A and B). PVCs and MVBs have been reported to function in the degradation, trafficking, and mobilization of various cellular components (23); thus, OsUCL23 might affect pollen intine development by regulating the function of these organelles.

To understand the role of OsUCL23 during microspore development, we then performed qRT-PCR using gene-specific primers to analyze its temporal expression pattern. WT anthers at the late microspore stage, early binucleate pollen stage, and late binucleate pollen stage were collected and used for an analysis of OsUCL23 and OsmiR528 expression. The results showed that OsUCL23 was expressed at low levels in the late binucleate pollen stage, during which the intine begins to accumulate (SI Appendix, Fig. S7A). OsmiR528 showed the opposite expression pattern to OsUCL23 (SI Appendix, Fig. S7A).  $\beta$ -Glucuronidase (GUS) activity analysis of OsmiR528 and OsUCL23 also showed that the promoter activity of OsmiR528 increased from the vacuolated stage to the mature stage, whereas OsUCL23 exhibited the opposite pattern and decreased beginning in the binucleate pollen stage (Fig. 4C and SI Appendix, Fig. S7B and C), indicating that OsmiR528 might function during sporogenesis. We further performed in situ hybridization of OsmiR528 and OsUCL23 to analyze their spatial expression patterns. Similar to the GUS signals, OsmiR528 gradually accumulated to a high level from the binucleate pollen stage to the mature stage, whereas the abundance of OsUCL23 mRNAs decreased during OsmiR528 accumulation (Fig. 4D). In addition, OsUCL23 mRNAs existed in both the pollen grains and tapetum, but OsmiR528 was expressed mainly in the pollen grains (Fig. 4D). These results indicated that OsmiR528-

mediated OsUCL23 degradation plays a role in intine development during the late binucleate pollen stage.

**OsUCL23 Interacts with a POT Family Protein to Regulate Flavonoid Metabolism.** To further demonstrate the molecular mechanisms by which OsUCL23 regulates the development of the pollen intine, we next identified OsUCL23-interacting proteins using a yeast 2-hybrid system and a rice young panicle cDNA library. Fragments from 6 proteins (LOC\_Os03g14610, LOC\_Os01g14670, LOC\_Os03g60840, LOC\_Os10g33170, LOC\_Os06g01210, and LOC\_Os03g17570) showed positive results. We further verified the interaction between the full-length proteins of the 6 genes and OsUCL23 protein, respectively, and only the POT protein (LOC\_Os10g33170) was proved to have authentically interacted with OsUCL23 (Fig. 5A). POT proteins are an evolutionarily conserved family of proton-coupled transport proteins spanning cellular membranes. A remarkable feature of the POT family is the diversity and extent of the natural substrates that they recognize. In mammals, fungi, and bacteria, POT proteins are predominantly peptide transporters, but in plants, the family has diverged to recognize nitrates, plant defense compounds, and hormones (26, 27). We hypothesized that OsUCL23 might interact with POT proteins on the membranes of PVCs and MVBs to mediate the transport of metabolites during pollen grain development.

To address this hypothesis, we first analyzed the subcellular localization of POT proteins in protoplasts. Similar to OsUCL23, POT showed perfect colocalization with the PVC/MVB marker VSR2 (Fig. 4B and SI Appendix, Fig. S6). To validate the in vivo interaction between the OsUCL23 and POT proteins, we then performed bimolecular fluorescence complementation (BiFC) in rice protoplasts. The results indicated that POT and OsUCL23 interact with each other in PVC/MVBs (Fig. 5A). We also analyzed the expression pattern of POT during anther development by in situ hybridization. The abundance of POT mRNAs was higher than that of OsmiR528 and OsUCL23 mRNAs, and they exhibited a similar expression pattern to OsUCL23 mRNAs (Fig. 4D). These mRNAs were highly accumulated at the vacuolated stage and decreased during pollen development in the pollen grains and tapetum (Fig. 4D), indicating similar roles for OsUCL23 and POT. The results showed that POT and OsUCL23 interact with each other in PVC/MVBs during early sporogenesis but decrease beginning in the binucleate pollen stage.

Second, to identify which metabolite may be affected by OsUCL23 and OsmiR528 in anthers, we performed 3 repetitions of high-throughput quantification of the metabolites present in WT, OXmiR528, mir528, ucl23, and OXUCL23 anthers at MPS, respectively, using a liquid chromatography-electrospray ionization-tandem mass spectrometry system and screened the metabolites that were the following: 1) complementarily changed between transgenic plants with higher OsUCL23 abundance (OXUCL23 and mir528) and those with lower OsUCL23 abundance (ucl23 and OXmiR528); 2) consistently changed between transgenic plants with a similar OsUCL23 expression pattern (OXUCL23 and mir528, ucl23, and OXmiR528). Among the 1,000 metabolic compounds detected in rice anthers, fewer than 200 were annotated. These metabolites included flavonoids, amino acids and their derivatives, fatty acids, nucleic acids and their derivatives, and other compounds. We analyzed only the changes in the levels of annotated metabolites. Following this standard, we screened 53 metabolites belonging to 14 classes, and 22 of them belonged to the flavonoid class, indicating that OsmiR528 and OsUCL23 mainly affected flavonoids. Among these 22 flavonoids, 17 were up-regulated in OXUCL23 anthers; 16 varied as expected in at least 3 samples; and 8 were up-regulated in both OXUCL23 and mir528 samples and down-regulated in both OXmiR528 and ucl23 samples, indicating that they might be directly regulated by OsmiR528 and OsUCL23 (SI Appendix, Fig. S7D). We further performed staining with the flavonol-specific dye diphenylboric acid-2-aminoethyl ester (DPBA) to monitor the accumulation pattern of flavonol in mutants and WT plants during anther development. DPBA staining showed that OXmiR528 and ucl23

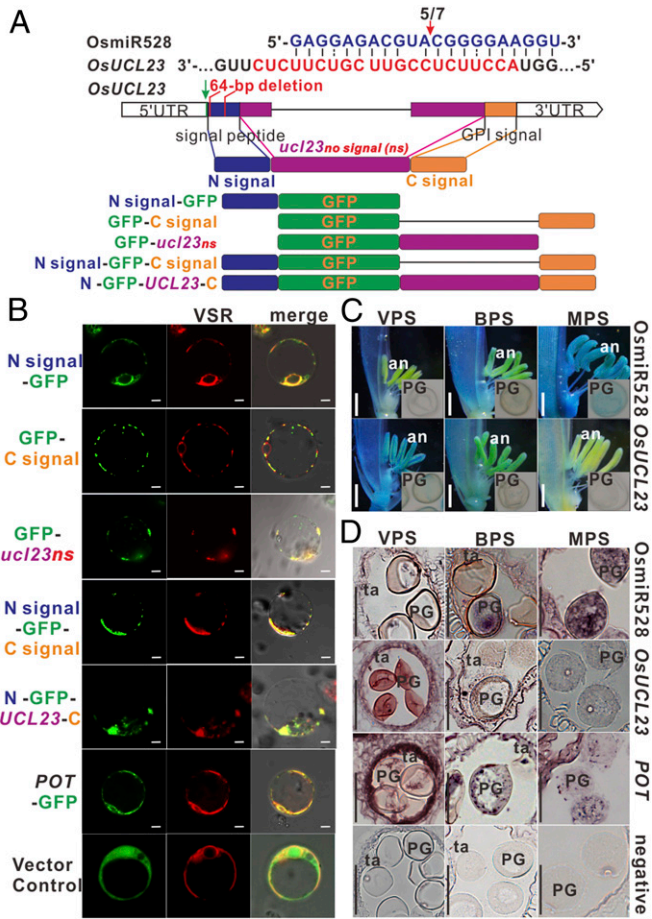


**Fig. 4.** The spatial and temporal expression patterns of *OsmiR528*, *OsUCL23*, and *POT* and their subcellular localizations. (A) Schematic representation of the *OsUCL23* gene structure, *OsmiR528* cleavage site, deletion generated by CRISPR-Cas9 in *ucl23*, and subcellular localization vectors of *OsUCL23*. (B) Subcellular localizations of different fusion proteins in which GFP was fused to different fragments of *OsUCL23* or to the C terminus of the *POT* protein. Green fluorescence represents the fusion proteins; red fluorescence represents the PVC/MVB marker. (Scale bars, 2 μm.) (C) Spatial expression pattern analysis of *OsmiR528* and *OsUCL23* in anthers during VPS, binucleate pollen stage (BPS), and MPS by GUS staining. The pollen grains are shown in the *Insets*. (Scale bars, 2 mm.) (D) In situ hybridization of *OsmiR528*, *OsUCL23*, and *POT* mRNAs at VPS, BPS, and MPS. PG, pollen grains; an, anthers; ta, tapetum. (Scale bars, 50 μm.)

pollen grains accumulated more flavonol at the binucleate pollen stage, but the flavonol content decreased to a lower level than in WT plants at the mature pollen stage, which was consistent with the metabolomics results, whereas OXUCL23 and *mir528* pollen grains showed opposite trends to those of the OXmiR528 and *ucl23* plants (Fig. 5B). Flavonols are required for pollen germination and tube growth and are constituents of the pollen wall (28, 29). Flavonoids are biosynthesized in the ER, and PVCs are involved in their transportation to other plant cell compartments, including the cytosol, vacuole, chloroplasts, and small vesicles (30). Our results showed that *OsmiR528* and *OsUCL23* regulate both flavonoid accumulation and intine deposition from the binucleate pollen stage to the mature pollen stage.

Finally, to verify whether *POT* plays a similar role to *OsUCL23* during pollen development and intine deposition, we constructed *POT* loss-of-function (*pot*) and *POT*-overexpressing (OX*POT*) transgenic plants (SI Appendix, Fig. S7 E and F). Phenotypic analysis indicated that the OX*POT* plants showed a similar (but more severe) phenotype to the OXUCL23 plants, where over half of the

pollen grains in OX*POT* anthers were nonviable and intine defective, and the seed-setting rate of OX*POT* was significantly lower than that of WT plants (Fig. 5 C–H). Thus, *pot* plants are similar to *ucl23* plants, which exhibit fewer aborted pollen grains and higher seed-setting rates than WT plants (Fig. 5 C–H). Taken together, our results indicate that *OsUCL23* interacts with a *POT* protein in PVC/MVBs, which together regulate intine deposition, pollen development, and seed-setting in rice.

**Discussion**

Unlike most miRNAs, *miR528* has evolved various functions in developmental regulation and stress responses by targeting distinct protein-coding genes (12–16). However, the functions of *miR528* in cleaving monocopper targets and fertility are unknown (31). In this study, we revealed that *OsmiR528* is essential for plant reproductive growth by targeting a monocopper target, *OsUCL23*. The *mir528* knockout mutant showed aborted pollen grains at the late binucleate pollen stage, which decreased its seed-setting rate. We showed that *OsmiR528* affects pollen development by directly targeting *OsUCL23* and regulating the deposition of the pollen intine. Taken together, our results add regulation of gametogenesis to the diverse known roles of *miR528*.

*OsUCL23* is a type-I arabinosylation (AGP) uclacyanin protein, which belongs to the phytoeyanin family. Compared with other phytoeyanins, uclacyanins are relatively small blue copper proteins that bind a single copper atom (32). Some members of the family are specifically localized in the cell plate and function in signal recognition and cell-wall biosynthesis. Treating *Nicotiana*

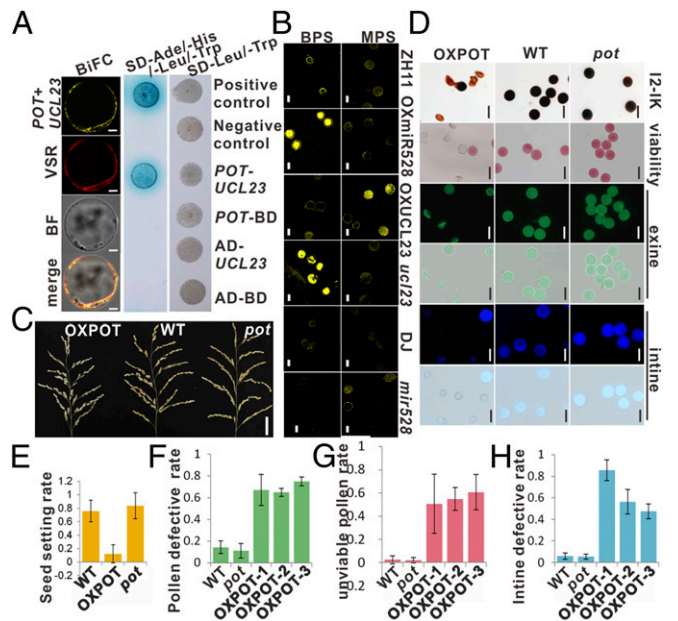


**Fig. 5.** Interaction of *OsUCL23* with a *POT* protein in PVC/MVBs and phenotypic analysis of *POT* gain-of-function and loss-of-function transgenic plants. (A) BiFC and yeast 2-hybrid analysis between *OsUCL23* and *POT*. For the yeast 2-hybrid analysis, the *POT* and *OsUCL23* open reading frames were fused in frame to pGBKT7 and pGADT7, respectively, to construct *POT*-BD and *AD*-*UCL23*. Both constructs were used to transform to the Y2HGold Yeast Strain (Clontech). Hybrids between *POT* and the pGBKT7 vector (*POT*-BD), the pGADT7 vector and *OsUCL23* (*AD*-*UCL23*), and the pGBKT7 vector and pGBKT7 vector (*AD*-BD) were used as negative controls. (Scale bars, 2 μm.) (B) DPBA staining showed that *OsUCL23* and *OsmiR528* regulate flavonoid contents at the BPS and MPS. (Scale bars, 25 μm.) (C) Panicles of OX*POT* and *pot* transgenic plants. (Scale bar, 4 cm.) (D) Histochemical staining of WT, OX*POT*, and *pot* pollen grains showed a defect in pollen grain maturation and the intine of the *pot* plants. (Scale bars, 50 μm.) (E–H) Statistical analysis of the seed-setting rate (E), pollen-defective rate (F), nonviable pollen rate (G), and intine-defective rate (H) of OX*POT* and *pot* plants. Values shown are the means ± SD (n > 10 plants, 200 pollen grains).

*tabacum* with a synthetic phenylglycoside that specifically binds AGPs decreased the normal asymmetric division of the zygote by affecting the accumulation of new cell-wall materials (33). These studies imply that AGPs affect the localization or transportation of new cell-wall components, regulating the formation of the primary cell wall during asymmetric cell divisions. In the present study, we showed that *OsUCL23* expressed in both pollen grains and tapetum and gradually down-regulated during sporogenesis and localized in the PVCs and MVBs. Plant MVBs and PVCs are single-membrane-bound organelles that are involved in secretory and trafficking in the endomembrane system in plants (23). They also are involved in plant reproductive development such as pollen tube growth and pollen tube–stigma interaction (34, 35). PVCs and MVBs were also reported to function in the formation of the primary cell wall and cell plates (36, 37). We inferred that *OsUCL23* might regulate the deposition of the intine by affecting PVC and MVB transportation, which is required for viable pollen grains.

We further identified a POT protein that interacted with *OsUCL23* in PVC/MVBs. POT family transporters represent one of the most promiscuous nutrient transport systems. In animals and bacteria, POT proteins are involved in the uptake of peptides for both metabolism and growth. Here, we showed that this protein colocalized with *OsUCL23* in PVC/MVBs, potentially forming a transporter complex to regulate metabolite transport. *OsmiR528* and *OsUCL23* could regulate the levels of flavonoids

and amino acids in the anthers. Flavonols are plant-specific compounds required for pollen germination and tube growth and are constituents of the pollen wall (28, 29). Previous studies have suggested that disordered intine formation would cause pollen tube burst (19). We propose that *OsUCL23* and the POT protein might form a transporter complex on the PVCs and MVBs and regulate pollen grain metabolism, particularly flavonoid transport, during pollen intine development. The study revealed the functions for *OsmiR528* and *uclacyanin* in pollen grain development.

## Materials and Methods

Detailed description is provided in *SI Appendix* for plant growth conditions, generation of transgenic rice plants, semithin sections, transmission electron microscopy, examination of gene expression by qRT-PCR analysis, Northern blot analysis, histochemical GUS staining, cytochemical analysis, metabolic profiling and transient expression assay, and BIFC.

**Data Availability.** The data that support the findings of this study are included in the main text and *SI Appendix*.

**ACKNOWLEDGMENTS.** We thank Ms. Q. J. Huang for technical support. This research was supported by the National Natural Science Foundation of China (Grants 91640202, 91940301, U1901202, and 31770883) and by Guangdong Province Grants 2016A030308015 and 2017TQ04N779) and Guangzhou Grant 201707020018.

1. T. Ariizumi, K. Toriyama, Genetic regulation of sporopollenin synthesis and pollen exine development. *Annu. Rev. Plant Biol.* **62**, 437–460 (2011).
2. J. K. Muhlemann, T. L. B. Younts, G. K. Muday, Flavonols control pollen tube growth and integrity by regulating ROS homeostasis during high-temperature stress. *Proc. Natl. Acad. Sci. U.S.A.* **115**, E11188–E11197 (2018).
3. C. Geserick, R. Tenhaken, UDP-sugar pyrophosphorylase is essential for arabinose and xylose recycling, and is required during vegetative and reproductive growth in *Arabidopsis*. *Plant J.* **74**, 239–247 (2013).
4. J. Li, M. Yu, L. L. Geng, J. Zhao, The fasciclin-like arabinogalactan protein gene, *FLA3*, is involved in microspore development of *Arabidopsis*. *Plant J.* **64**, 482–497 (2010).
5. S. Moon *et al.*, Rice glycosyltransferase1 encodes a glycosyltransferase essential for pollen wall formation. *Plant Physiol.* **161**, 663–675 (2013).
6. M. Sumiyoshi *et al.*, UDP-arabinopyranose mutase 3 is required for pollen wall morphogenesis in rice (*Oryza sativa*). *Plant Cell Physiol.* **56**, 232–241 (2015).
7. L. G. Rydén, L. T. Hunt, Evolution of protein complexity: The blue copper-containing oxidases and related proteins. *J. Mol. Evol.* **36**, 41–66 (1993).
8. S. Kim *et al.*, Chemocyanin, a small basic protein from the lily stigma, induces pollen tube chemotropism. *Proc. Natl. Acad. Sci. U.S.A.* **100**, 16125–16130 (2003).
9. J. Dong, S. T. Kim, E. M. Lord, Plantacyanin plays a role in reproduction in *Arabidopsis*. *Plant Physiol.* **138**, 778–789 (2005).
10. R. Sunkar, J. K. Zhu, Novel and stress-regulated microRNAs and other small RNAs from *Arabidopsis*. *Plant Cell* **16**, 2001–2019 (2004).
11. J. P. Zhang *et al.*, *MiR408* regulates grain yield and photosynthesis via a phytochrome protein. *Plant Physiol.* **175**, 1175–1185 (2017).
12. S. Yuan *et al.*, Constitutive expression of rice *MicroRNA528* alters plant development and enhances tolerance to salinity stress and nitrogen starvation in creeping bentgrass. *Plant Physiol.* **169**, 576–593 (2015).
13. Q. Liu *et al.*, Involvement of *miR528* in the regulation of arsenite tolerance in rice (*Oryza sativa* L.). *J. Agric. Food Chem.* **63**, 8849–8861 (2015).
14. J. Wu *et al.*, ROS accumulation and antiviral defence control by *microRNA528* in rice. *Nat. Plants* **3**, 16203 (2017).
15. S. Yao *et al.*, Transcriptional regulation of *miR528* by *OsSPL9* orchestrates antiviral response in rice. *Mol. Plant* **12**, 1114–1122 (2019).
16. R. Yang *et al.*, Fine-tuning of *MiR528* accumulation modulates flowering time in rice. *Mol. Plant* **12**, 1103–1113 (2019).
17. H. Zhang *et al.*, Small RNA profiles of the rice PTGMS line wuxiang 5 reveal miRNAs involved in fertility transition. *Front. Plant Sci.* **7**, 514 (2016).
18. J. S. Jeon *et al.*, T-DNA insertional mutagenesis for functional genomics in rice. *Plant J.* **22**, 561–570 (2000).
19. J. Jiang *et al.*, PECTATE LYASE-LIKE 9 from *Brassica campestris* is associated with intine formation. *Plant Sci.* **229**, 66–75 (2014).
20. M. Lin, E. He, D. Wei, H. Tian, ATPase changes in rice anthers. *Int. J. Plant Dev. Biol.* **3**, 39–46 (2009).
21. S. Ishikawa *et al.*, Suppression of tiller bud activity in tillering dwarf mutants of rice. *Plant Cell Physiol.* **46**, 79–86 (2005).
22. M. G. Paulick, C. R. Bertozzi, The glycosylphosphatidylinositol anchor: A complex membrane-anchoring structure for proteins. *Biochemistry* **47**, 6991–7000 (2008).
23. Y. Cui *et al.*, Biogenesis of plant prevacuolar multivesicular bodies. *Mol. Plant* **9**, 774–786 (2016).
24. S. K. Lam *et al.*, BFA-induced compartments from the Golgi apparatus and trans-Golgi network/early endosome are distinct in plant cells. *Plant J.* **60**, 865–881 (2009).
25. C. Hachez *et al.*, *Arabidopsis* SNAREs *SYP61* and *SYP121* coordinate the trafficking of plasma membrane aquaporin *PIP2;7* to modulate the cell membrane water permeability. *Plant Cell* **26**, 3132–3147 (2014).
26. J. L. Parker *et al.*, Proton movement and coupling in the POT family of peptide transporters. *Proc. Natl. Acad. Sci. U.S.A.* **114**, 13182–13187 (2017).
27. S. Newstead, Recent advances in understanding proton coupled peptide transport via the POT family. *Curr. Opin. Struct. Biol.* **45**, 17–24 (2017).
28. V. N. Guyon, J. D. Astwood, E. C. Garner, A. K. Dunker, L. P. Taylor, Isolation and characterization of cDNAs expressed in the early stages of flavonol-induced pollen germination in petunia. *Plant Physiol.* **123**, 699–710 (2000).
29. C. Fellenberg, T. Vogt, Evolutionarily conserved phenylpropanoid pattern on angiosperm pollen. *Trends Plant Sci.* **20**, 212–218 (2015).
30. E. Petrusa *et al.*, Plant flavonoids: Biosynthesis, transport and involvement in stress responses. *Int. J. Mol. Sci.* **14**, 14950–14973 (2013).
31. C. Chen, Y. Liu, R. Xia, Jack of many trades: The multifaceted role of *miR528* in monocots. *Mol. Plant* **12**, 1044–1046 (2019).
32. H. Ma, H. Zhao, Z. Liu, J. Zhao, The phytochrome gene family in rice (*Oryza sativa* L.): Genome-wide identification, classification and transcriptional analysis. *PLoS One* **6**, e25184 (2011).
33. Y. Qin, J. Zhao, Localization of arabinogalactan proteins in egg cells, zygotes, and two-celled proembryos and effects of beta-D-glucosyl Yariv reagent on egg cell fertilization and zygote division in *Nicotiana tabacum* L. *J. Exp. Bot.* **57**, 2061–2074 (2006).
34. H. Wang *et al.*, Vacuolar sorting receptors (VSRs) and secretory carrier membrane proteins (SCAMPs) are essential for pollen tube growth. *Plant J.* **61**, 826–838 (2010).
35. L. Hao, J. Liu, S. Zhong, H. Gu, L. J. Qu, AtVPS41-mediated endocytic pathway is essential for pollen tube-stigma interaction in *Arabidopsis*. *Proc. Natl. Acad. Sci. U.S.A.* **113**, 6307–6312 (2016).
36. M. S. Otegui, D. N. Mastrorade, B. H. Kang, S. Y. Bednarek, L. A. Staehelin, Three-dimensional analysis of syncytial-type cell plates during endosperm cellularization visualized by high resolution electron tomography. *Plant Cell* **13**, 2033–2051 (2001).
37. C. M. Chow, H. Neto, C. Foucart, I. Moore, Rab-A2 and Rab-A3 GTPases define a trans-golgi endosomal membrane domain in *Arabidopsis* that contributes substantially to the cell plate. *Plant Cell* **20**, 101–123 (2008).